

Overcoming “Coffee-Stain” Effect by Compositional Marangoni Flow Assisted Drop-Drying

Mainak Majumder^{1,2}, Clint S. Rendall¹, J. Alexander Eukel¹, James Y.L. Wang¹, Natnael Behabtu¹, Cary L. Pint³, Tzu-Yu Liu¹, Alvin W. Orbaek³, Francesca Mirri¹, Jaewook Nam¹, Andrew R. Barron^{3,4}, Robert H. Hauge^{3,4}, Howard K. Schmidt^{3,4}, Matteo Pasquali^{1,3,4}*

¹Department of Chemical & Biomolecular Engineering, Rice University, Houston, TX-77005

²Nanoscale Science and Engineering Laboratory (NSEL), Department of Mechanical and Aerospace Engineering, Monash University, Clayton, VIC-3800

³Department of Chemistry, Rice University, Houston, TX- 77005

⁴The Smalley Institute for Nanoscale Science & Technology, Rice University,
Houston, TX- 77005

*E-mail: mp@rice.edu

S1. Synthesis and Characterization of Fe oxide and FeCo oxide nanoparticles

All materials were purchased from Sigma-Aldrich and used as received. Nanoparticle synthesis of the Fe oxide nanoparticles was carried out in a 100 ml 3 neck round-bottomed flask, 0.75 mmol Fe(acac)₃, 1.5 mmol 1,2-hexadecanediol, 3 mmol oleic acid, 4 mmol oleyl amine, and 37.5 mL benzyl ether. This was brought to reflux under inert condition for a period of 15 minutes, after cooling to room temperature the solution is precipitated in EtOH, then centrifuged for 5 min at 4400 rpm. The supernatant was discarded and the pellet made soluble in approximately 10 mL of Hexanes using light bath sonication to ensure solubility. The FeCo oxide nanoparticles were made in the same fashion using instead 0.5 mmol Fe(acac)₃ and 0.25 mmol Co(acac)₂, and a total of 3 mmol oleyl amine and 3 mmol oleic acid.

Size was then determined by small angle x-ray scattering (SAXS) on a Rigaku SmartLab X-Ray diffractometer using a Cu-K α radiation source. Samples were analyzed using 1 mm “Glass Number 50 Capillary” tubes (Hampton Research Inc). The data was resolved using Rigaku’s NANO-solver. The sizes for the nanoparticles were 7 nm and 5 nm in diameter for the iron oxide and FeCo oxide respectively. This solution was then added to a 10% Igepal solution in ratios of 1:1, 1:2, and 1:4. For example, a total of 50 mL solution was bath sonicated for a period of 6 minutes at 30 % power with a frequency of 1 sec on, 2 sec off. From this treatment the emulsion requires approximately two days to stabilize. The FeCo alloy nanoparticles were mixed in a 1:4 ratio and the Fe nanoparticles were mixed at various ratios to acquire a range of concentrations. It should be noted that the lids are left such that hexanes can evaporate out of solution, as such it

would be expected that there is not any hexanes in the water solution of the stable emulsion after the two days.

Concentration was determined by inductively coupled plasma-atomic emission spectroscopy (ICP-AES) measurements using a Perkin Elmer Optima 4300DV. The analyte was prepared using a 25% solution of chloric acid solution to digest the igepal polymer, these were then further digested in fixed amounts of concentrated Nitric acid. Typically the samples were prepared by digesting 100 μ L nanoparticle polymer solution in 200 μ L chloric acid, the mixture was then heated until completely dry. Then 0.5 mL concentrated nitric acid was used to re-dissolve the metals into solution, this was then diluted to a 7% nitric acid solution by the addition of an appropriate amount of nanopure water and subsequently. ICP-AES concentrations were calibrated using standards from Inorganic Ventures and subsequently diluted using nanopure water. In the case of the FeCo nanoparticles the iron content was accumulated separately to the cobalt in order to avoid wavelength overlap between their respective signals. The FeCo particle emulsion mixed with a (1:4 np:igepal soln) was found to have a concentration of 2152 ppm of Iron. For the Iron oxide particles the concentrations increased in a linear fashion according increasing nanoparticle content in the the ratio of np:igepal solution. 1:4, 1:2, and 1:1 solution achieved Fe concentrations of 2208, 3898, and 6972 ppm respectively. Figure S1 shows the variation of color in the solution with respect to change in the concentration of nanoparticles and igepal. The original iron oxide nanoparticles used to dissolve in igepal, and the np:igepal solution of 1:4 ratio that grew SWNT carpets were imaged using an Hitachi S-5500 Hi-Res SEM as shown in figure S1.

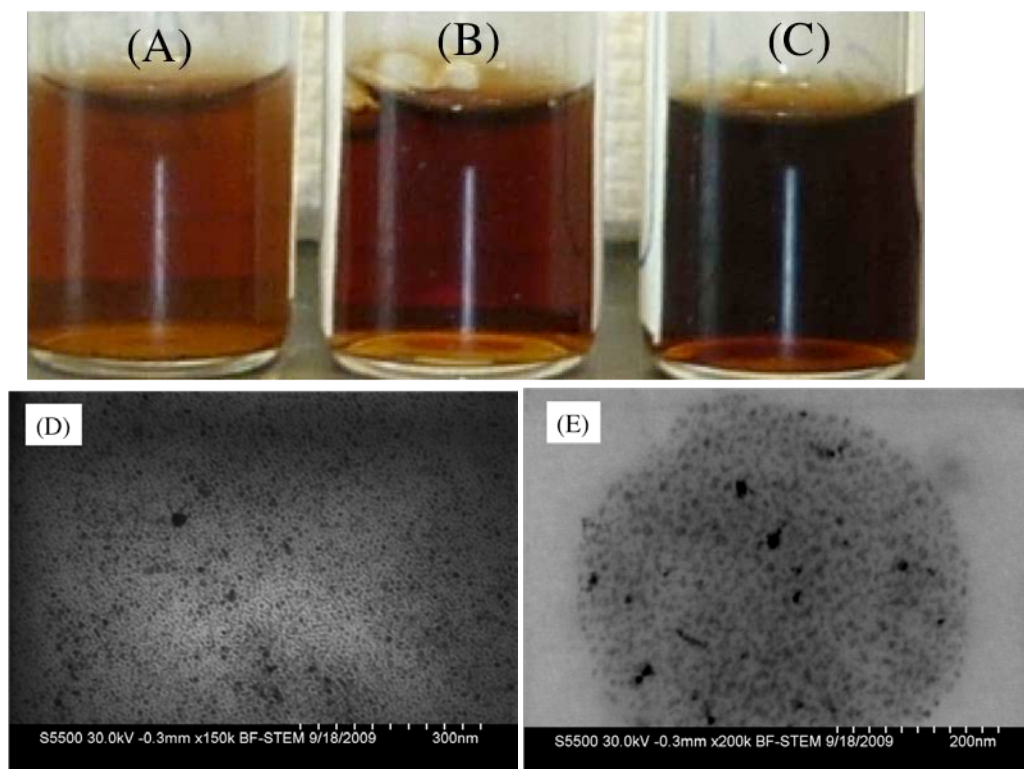


Figure S1: Picture showing the colors of the iron oxide nanoparticles in igeal solution for three concentrations, (A) 2208 ppm Fe, (B) 3898 ppm Fe, and (C) 6972 ppm Fe. With STEM images of (D) the iron oxide nanoparticles, and (E) STEM image of sample (C) showing the iron oxide nanoparticles now aggregated together by the igeal polymer.

S2. Characterization of Au-nanoparticle suspension and deposition on glass substrates

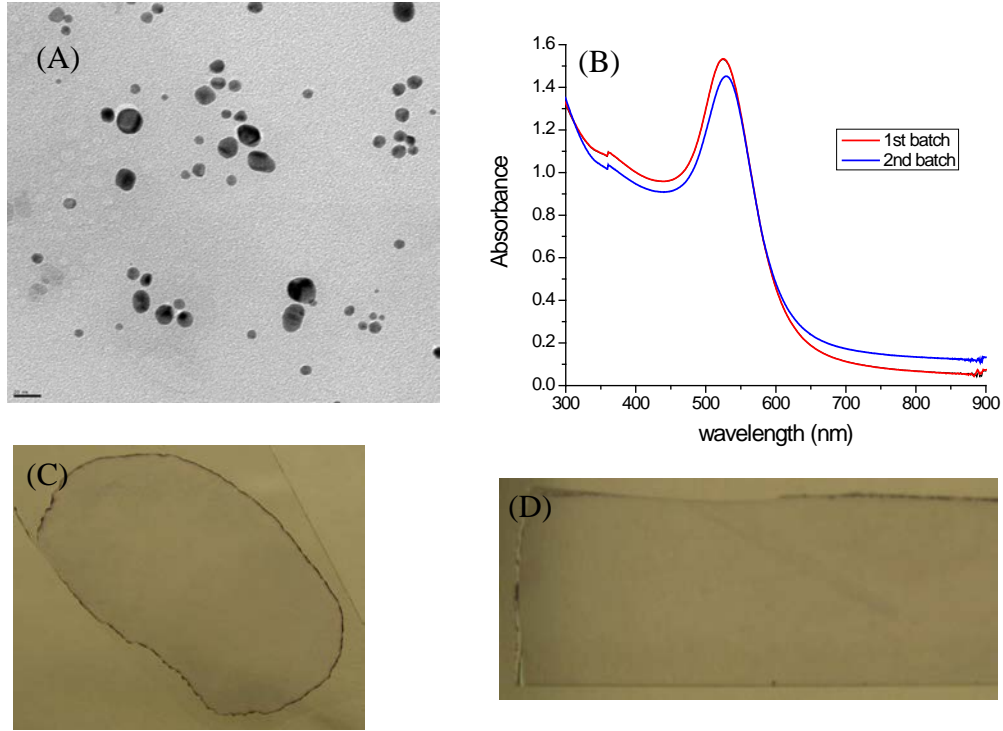


Figure S2: (A) TEM images of Au-nanoparticle synthesized in our laboratory. (B) UV-vis spectra of the solution shows a peak at ~ 529 nm. Photographs of Au-nanoparticle deposition on a glass substrate: (C) dried in air, (D) dried in ethanol vapor atmosphere

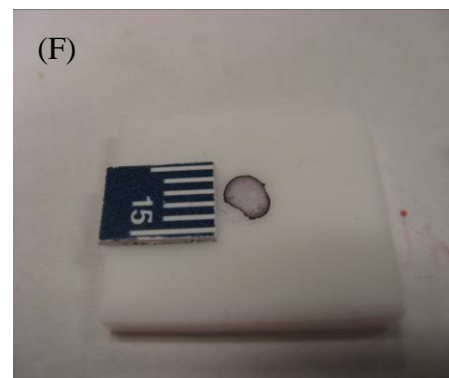
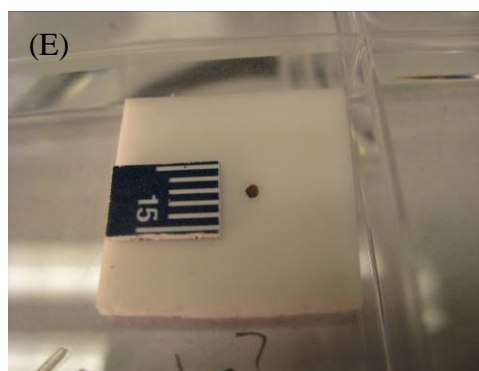
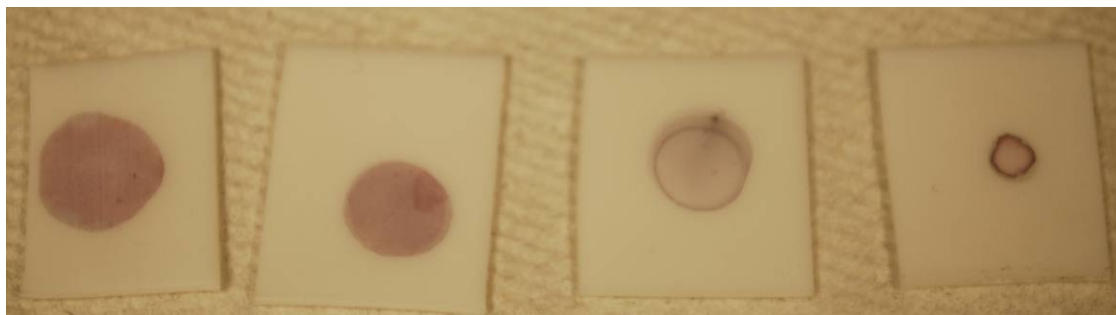
S3. Visualization of internal droplet flow

Fluid motion within a water droplet was visualized using tracer particles (Polybead Black Dyed Microspheres (Polysciences Inc. with a diameter of ~ 3 μm and ~ 10 μm). A CCD camera (Photometrics CoolSnap cf) with microscopic lens captured the movies. We optimized the concentration such that light would pass easily through the

droplet, yet there were enough microspheres for easy observation. This concentration was found to be $\sim 1 \mu\text{l}$ of microspheres per 10 ml of deionized water. With the camera mounted horizontally, the Petri dish is placed on a stand of variable height approximately 5 cm away. Once the droplet has been placed on the surface of interest, the height of the stand is then adjusted to provide a clear and complete picture. It was also found that slightly tilting the Petri dish in the direction of the camera – no more than $5\text{-}10^\circ$ – produced superior image quality. The first video (jp3009628_si_002.avi) is presented at 60 times faster than real time, while the second (jp3009628_si_003.avi) is 13 times faster. The colors in these videos were inverted and contrast was enhanced for particulate clarity.

S4. Photographs of Marangoni and air-dried drops on Teflon surface

Drops ($\sim 5 \mu\text{l}$) of Au-nanoparticle were dried on a Teflon[®] surface and dried under saturated environments of methanol, ethyl alcohol, and isopropyl alcohol (figures S4(A) through S4(C)) and is compared against drop dried under ambient conditions - figure S4(D)).



Photographs of the drops dried under water vapor atmosphere is shown in Figure S4(E) and under ambient conditions after ~ 45 minutes of spreading under saturated ethanol atmosphere is shown in Figure S4(F)

Figure S4. Photographs of 5 μ l Au-nanoparticle suspensions dried under atmospheres of (A) methanol; (B) ethanol; (C) iso-propyl alcohol; and (D) air; Photographs of 5 μ l of Au-nanoparticle suspension: (E) dried in water vapor atmosphere; (F) dried under ambient after ~ 45 minutes spreading under an ethanol vapor atmosphere.

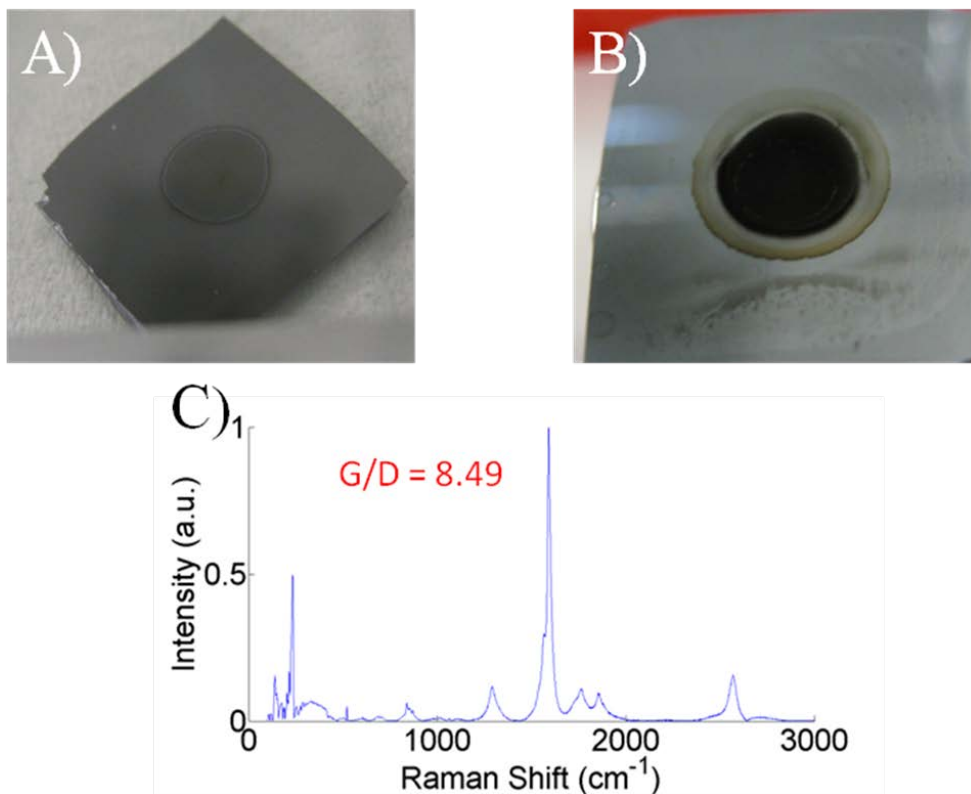


Figure S5: Applications of the Marangoni-assisted nano-particle deposition technique for growth of single walled carbon nanotubes grown from Fe-Co nanoparticles deposited on HMDS functionalized Si substrate, dried under Marangoni drying conditions with acetic acid as co-solvent. (A) Before growth; (B) after growth. (C) Normalized Raman spectrum at three different locations.